Nonlinear Dyn (2010) 62: 769–779
DOI 10.1007/s11071-010-9761-z

ORIGINAL PAPER

Nonlinear modeling and control of flexible-link manipulators subjected to parametric excitation

Ayman A. El-Badawy · Mohamed W. Mehrez · Amir R. Ali

Received: 12 October 2009 / Accepted: 9 June 2010 / Published online: 9 July 2010

Abstract This paper presents nonlinear dynamic modeling and control of flexible-link manipulators subjected to parametric excitation. The equations of motion are obtained using the Lagrangian-assumed modes method. Singular perturbation methodology is developed for the nonlinear time varying equations of motion to obtain a reduced-order set of equations. Control strategies, computed torque control and a composite control, based on the singular perturbation formulation developed, are utilized to reduce mechanical vibrations of the flexible-link and enable better tip positioning. Under the composite control technique, the effect of the value of perturbation parameter on the control signal is investigated. Numerical simulations supported by real-time experiments show that the singular-perturbation control methodology developed for the nonlinear time-varying system offers better system response over the computed torque control as the manipulator is commanded to follow a certain trajectory.

A.A. El-Badawy (✉) · M.W. Mehrez · A.R. Ali
Faculty of Engineering and Material Science,
The German University in Cairo, Cairo, Egypt
e-mail: ayman.elbadawy@guc.edu.eg

M.W. Mehrez
e-mail: mohamed.waleed@guc.edu.eg

A.R. Ali
e-mail: amir.ali@guc.edu.eg

Keywords Parametric excitation · Flexible manipulator · Computed torque · Singular perturbation · Composite control · Perturbation parameter

1 Introduction

The performance of a robotic manipulator mounted on a crane, mobile platform, or an autonomous vehicle is affected by base excitation. The oscillating base can be modeled as a spring–mass–damper system and thus a new degree of freedom is added to the system. Alternatively, the oscillation of the base can be considered as parametric excitation, where the excitation appears as coefficients in the governing differential equations [1]. The difference between the two modeling strategies is that in the first one the control objective is to achieve suppression of base oscillations [2]. In the second case, the control objective is to reduce the vibrations of the flexible link and maintain the accuracy of the tip position in the presence of sustained parametric excitation.

Young and Moon [3] used a simple robust control strategy that reduces mechanical vibrations of the base and enables better tip positioning. The control algorithm uses the sensory feedback of the base oscillation to modulate the manipulator actuator input to induce the inertial damping forces. Active damping control problems of robot manipulators with oscillatory bases

are considered by Lin et al. [2], where a first investigation of two-time scale fuzzy logic controller with vibration stabilizer for such structures has been proposed. Lin and Huang [4] proposed a new hierarchical fuzzy logic controller of mechanical systems with oscillatory bases, where the dynamics of a robotic system is strongly affected by disturbances due to the base oscillation. In the above literature, the robotic manipulator mounted on the oscillating-base is considered to be rigid.

In contrast, flexible robot manipulators exhibit many advantages over their rigid counterparts: they require less material, are lighter in weight, have higher manipulation speed, are more maneuverable and transportable, are safer to operate, have less overall cost and higher payload-to-robot-weight ratio [5]. However, the problems due to the distributed link flexibility and the resulting vibrations often lead to long settling times and position inaccuracy in lightweight manipulators. Hence, it is essential to develop comprehensive dynamic models for this type of manipulator that consider all these factors. This will enable improved control techniques to be devised so that performance can be optimized [6]. A review of the dynamic analyses of flexible manipulators attached to fixed bases is presented by Dwivedy and Eberhard [7], where the authors examined the methods used in these analyses, their advantages and shortcomings and possible extensions of these methods to be applied to a general problem. Ider et al. [8] developed a full-state feedback control after linearizing the dynamic equations of a two-link robot with flexible links. A model of N-link flexible manipulators is derived and reformulated in the form of singular perturbation theory and an integral manifold is used to separate fast dynamics from slow dynamics. A composite control algorithm [9] is proposed for the flexible robots, which consists of two main parts. Fast control, u_f, guarantees that the fast dynamics remains asymptotically stable. Slow control, u_s, consists of a robust PD designed based on the rigid model.

In this work, the dynamic equations of motion of flexible manipulators subjected to parametric excitation are presented. Two control techniques are used to investigate the response of such systems, computed torque control [10] and a composite control based on singular perturbation theory [11]. The effect of the value of the perturbation parameter on the composite control method is investigated and then utilized to improve the system response while minimizing the control effort. A study on a one-link flexible arm is carried out. Theoretical results and real-time experiments show that composite control offers better system response than that using computed torque control when the manipulator is commanded to follow a certain trajectory.

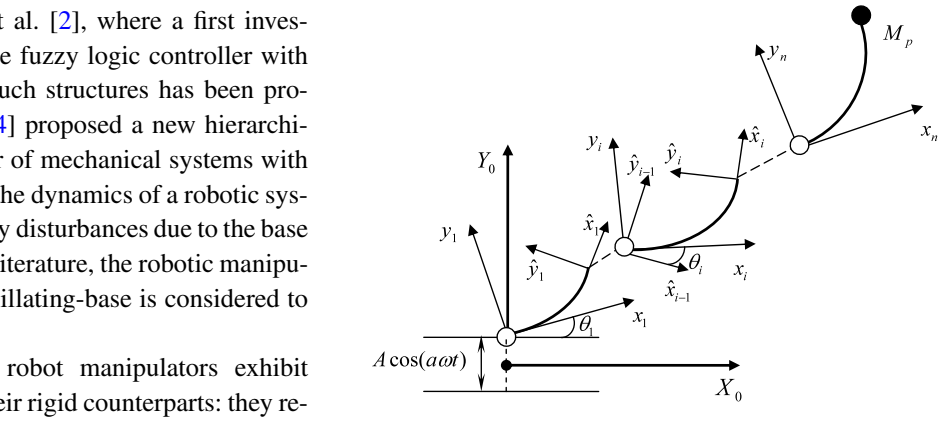

Fig. 1 Multi-link flexible manipulator subjected to parametric excitation

2 Nonlinear equations of motion

Consider the manipulator shown in Fig. 1. It is a multi-link flexible arm with rotary joints that moves in the horizontal plane. The transformation matrix $\mathbf{T}_i$ between frame i and the inertial frame is [12]

$$\mathbf{T}_i = \mathbf{T}_{i-1}\mathbf{E}_{i-1}\mathbf{A}_i. \tag{1}$$

Here, $\mathbf{A}_i$ is the joint transformation matrix for joint i due to rigid motion, $\mathbf{E}_i$ is the link transformation matrix for link $i-1$ between joints $i-1$ and i due to its length and deflection. And the parametric excitation term is included in $\mathbf{T}_1$ as:

$$\mathbf{T}_1 = \begin{bmatrix} \cos(\theta_1) & -\sin(\theta_1) & 0 & 0 \\ \sin(\theta_1) & \cos(\theta_1) & 0 & A\cos(a\omega t) \\ 0 & 0 & 1 & 0 \\ 0 & 0 & 0 & 1 \end{bmatrix}, \tag{2}$$

and the transformation $\mathbf{E}_i$ is given as

$$\mathbf{E}_i = \begin{bmatrix} 1 & v'_{ie}(x_i,t) & 0 & l_i \\ v'_{ie}(x_i,t) & 1 & 0 & 0 \\ 0 & 0 & 1 & 0 \\ 0 & 0 & 0 & 1 \end{bmatrix}, \tag{3}$$

where $v(x_i,t)$ denotes the transversal deformation of link i, $v'_{ie}(x_i,t) = \frac{\partial v_i(x_i,t)}{\partial x_i}|_{x_i=l_i}$, and the linear approximation $\arctan(v'_{ie}(x_i,t)) \approx v'_{ie}(x_i,t)$ is valid for small deflections.

Using total kinetic energy and total potential energy of the flexible manipulator, the equations of motion of the manipulator can be obtained using a combined Lagrange-assumed modes approach [12, 13]. The equations of motion of an n-link flexible arm, with m_i being the number of modes used to describe the deflection of link i, can be written in the form [9]

$$\mathbf{M}(\boldsymbol{\theta},\boldsymbol{\delta}) \begin{bmatrix} \ddot{\boldsymbol{\theta}} \\ \ddot{\boldsymbol{\delta}} \end{bmatrix} + \begin{bmatrix} \mathbf{f}_1(\boldsymbol{\theta},\dot{\boldsymbol{\theta}},t) \\ \mathbf{f}_2(\boldsymbol{\theta},\dot{\boldsymbol{\theta}},t) \end{bmatrix} + \begin{bmatrix} \mathbf{g}_1(\boldsymbol{\theta},\dot{\boldsymbol{\theta}},\boldsymbol{\delta},\dot{\boldsymbol{\delta}},t) \\ \mathbf{g}_2(\boldsymbol{\theta},\dot{\boldsymbol{\theta}},\boldsymbol{\delta},\dot{\boldsymbol{\delta}},t) \end{bmatrix} + \begin{bmatrix} \mathbf{0} \\ \mathbf{K}\boldsymbol{\delta} \end{bmatrix} = \begin{bmatrix} \mathbf{T} \\ \mathbf{0} \end{bmatrix}, \tag{4}$$

where $\mathbf{M} = \begin{bmatrix} \mathbf{M}^{rr} & \mathbf{M}^{re} \\ \mathbf{M}^{er} & \mathbf{M}^{ee} \end{bmatrix}$ is the inertia matrix, superscripts r and e refer to rigid body (joint) and elastic degrees of freedom, respectively. $\boldsymbol{\theta} = [\theta_1 \ \dots \ \theta_n]^{\mathrm{T}}$ is the vector of joint variables, $\boldsymbol{\delta} = [\delta_{11} \ \dots \ \delta_{1m_1} \ \delta_{21} \ \dots \ \delta_{2m_n}]^{\mathrm{T}}$ is the vector of deflection variables, $\mathbf{f}_1$ and $\mathbf{f}_2$ are the vectors containing gravitational, Coriolis, and centrifugal terms, $\mathbf{g}_1$ and $\mathbf{g}_2$ are the vectors which account for the interaction of joint variables and their time derivatives with deflection variables and their time derivatives, $\mathbf{K}$ is a diagonal matrix whose diagonal sub-matrices are the stiffness matrices of links in terms of the deflection variables, and $\mathbf{u} = [\mathbf{T}\ \mathbf{0}]^{\mathrm{T}}$, where $\mathbf{T}$ is the vector of joints torques. As an effect of parametric excitation, the vectors $\mathbf{f}_1$, $\mathbf{f}_2$, $\mathbf{g}_1$, and $\mathbf{g}_2$ are functions of time as well as $\boldsymbol{\theta}$ and $\boldsymbol{\delta}$ and their time derivates, which is not the case when the parametric excitation is not considered.

Since the inertia matrix $\mathbf{M}$ is positive definite, it can be inverted and denoted by $\mathbf{H}$, which can be partitioned as follows:

$$\mathbf{M}^{-1} = \mathbf{H} = \begin{bmatrix} \mathbf{H}_{11[n\times n]} & \mathbf{H}_{12[n\times m]} \\ \mathbf{H}_{21[m\times n]} & \mathbf{H}_{22[m\times m]} \end{bmatrix} \tag{5}$$

Now, (4) become

$$\ddot{\boldsymbol{\theta}} = -\mathbf{H}_{11}\mathbf{f}_1 - \mathbf{H}_{12}\mathbf{f}_2 - \mathbf{H}_{11}\mathbf{g}_1 - \mathbf{H}_{12}\mathbf{g}_2 - \mathbf{H}_{12}\mathbf{K}\boldsymbol{\delta} + \mathbf{H}_{11}\mathbf{T}, \tag{6a}$$

$$\ddot{\boldsymbol{\delta}} = -\mathbf{H}_{21}\mathbf{f}_1 - \mathbf{H}_{22}\mathbf{f}_2 - \mathbf{H}_{21}\mathbf{g}_1 - \mathbf{H}_{22}\mathbf{g}_2 - \mathbf{H}_{22}\mathbf{K}\boldsymbol{\delta} + \mathbf{H}_{21}\mathbf{T}. \tag{6b}$$

The flexible dynamic system (6a) and (6b) is characterized by $n+m$ generalized coordinates but only n control inputs. Therefore, the synthesis of a nonlinear feedback control is not as easy as for a rigid arm (a control input for each joint).

A model order reduction is made by the use of singular perturbation theory, leading to a composite control for the full order system [14]. The reduced order system is presented in the next section.

3 Flexible arm control

In this section, two control techniques are presented: the computed torque control and a composite control based on the singular perturbation approach. The computed torque control [10] is a common control technique that is used for rigid manipulators, where the control signal is computed through

$$\mathbf{T} = \mathbf{M}^{rr}\left[\ddot{\boldsymbol{\theta}}_d + \mathbf{k}_v(\dot{\boldsymbol{\theta}}_d - \dot{\boldsymbol{\theta}}) + \mathbf{k}_p(\boldsymbol{\theta}_d - \boldsymbol{\theta})\right] + \mathbf{f}_1, \tag{7}$$

where in $\mathbf{M}^{rr}$ and $\mathbf{f}_1$, $\boldsymbol{\delta}$'s are set to zero. $\mathbf{k}_v$ and $\mathbf{k}_p$ are the velocity and position feedback gain diagonal matrices, respectively. $\boldsymbol{\theta}_d, \dot{\boldsymbol{\theta}}_d$, and $\ddot{\boldsymbol{\theta}}_d$ are the desired trajectory position, velocity, and acceleration respectively. In the following subsections, a composite control based on singular perturbation approach is derived.

3.1 A singularly perturbed model

A singularly perturbed model of the dynamic system (6) can be obtained as follows. Assuming that the orders of magnitude of the $\mathbf{K}$ matrix elements (k_i's) are comparable, it is appropriate to extract a common scale factor $1/\mu$ (where μ is the perturbation parameter) such that

$$k_i = (1/\mu)\tilde{k}_i, \quad i = 1,\dots,m. \tag{8}$$

The following new variables (elastic forces) can be defined:

$$\boldsymbol{\zeta} = (1/\mu)\tilde{\mathbf{k}}\boldsymbol{\delta}, \tag{9}$$

$$\tilde{\mathbf{k}} = \operatorname{diag}(\tilde{k}_1 \ \ldots \ \tilde{k}_m). \tag{10}$$

Now, (6) can be written as

$$\begin{aligned}\ddot{\boldsymbol{\theta}} = &-\mathbf{H}_{11}(\boldsymbol{\theta}, \mu\boldsymbol{\zeta})\mathbf{f}_1(\boldsymbol{\theta}, \dot{\boldsymbol{\theta}}, t) - \mathbf{H}_{12}(\boldsymbol{\theta}, \mu\boldsymbol{\zeta})\mathbf{f}_2(\boldsymbol{\theta}, \dot{\boldsymbol{\theta}}, t)\\ &- \mathbf{H}_{11}(\boldsymbol{\theta}, \mu\boldsymbol{\zeta})\mathbf{g}_1(\boldsymbol{\theta}, \dot{\boldsymbol{\theta}}, \mu\boldsymbol{\zeta}, \mu\dot{\boldsymbol{\zeta}}, t)\\ &- \mathbf{H}_{12}(\boldsymbol{\theta}, \mu\boldsymbol{\zeta})\mathbf{g}_2(\boldsymbol{\theta}, \dot{\boldsymbol{\theta}}, \mu\boldsymbol{\zeta}, \mu\dot{\boldsymbol{\zeta}}, t)\\ &- \mathbf{H}_{12}(\boldsymbol{\theta}, \mu\boldsymbol{\zeta})\boldsymbol{\zeta} + \mathbf{H}_{11}(\boldsymbol{\theta}, \mu\boldsymbol{\zeta})\mathbf{T},\end{aligned} \tag{11a}$$

$$\begin{aligned}\mu\ddot{\boldsymbol{\zeta}} = &-\mathbf{H}_{21}(\boldsymbol{\theta}, \mu\boldsymbol{\zeta})\mathbf{f}_1(\boldsymbol{\theta}, \dot{\boldsymbol{\theta}}, t) - \mathbf{H}_{22}(\boldsymbol{\theta}, \mu\boldsymbol{\zeta})\mathbf{f}_2(\boldsymbol{\theta}, \dot{\boldsymbol{\theta}}, t)\\ &- \mathbf{H}_{21}(\boldsymbol{\theta}, \mu\boldsymbol{\zeta})\mathbf{g}_1(\boldsymbol{\theta}, \dot{\boldsymbol{\theta}}, \mu\boldsymbol{\zeta}, \mu\dot{\boldsymbol{\zeta}}, t)\\ &- \mathbf{H}_{22}(\boldsymbol{\theta}, \mu\boldsymbol{\zeta})\mathbf{g}_2(\boldsymbol{\theta}, \dot{\boldsymbol{\theta}}, \mu\boldsymbol{\zeta}, \mu\dot{\boldsymbol{\zeta}}, t)\\ &- \mathbf{H}_{22}(\boldsymbol{\theta}, \mu\boldsymbol{\zeta})\boldsymbol{\zeta} + \mathbf{H}_{21}(\boldsymbol{\theta}, \mu\boldsymbol{\zeta})\mathbf{T},\end{aligned} \tag{11b}$$

which is a singularly perturbed model of the flexible arm. Notice that all quantities on the right-hand side of (11b) have been conveniently scaled by $\tilde{\mathbf{k}}$.

It can be shown that as $\mu = 0$, the model of the rigid manipulator is obtained from (11a) and (11b). Formally, setting $\mu = 0$ and solving for $\boldsymbol{\zeta}$ in (11b), one obtains

$$\begin{aligned}\bar{\boldsymbol{\zeta}} = &\mathbf{H}_{22}^{-1}(\bar{\boldsymbol{\theta}}, 0)\big[-\mathbf{H}_{21}(\bar{\boldsymbol{\theta}}, 0)\mathbf{f}_1(\bar{\boldsymbol{\theta}}, \dot{\bar{\boldsymbol{\theta}}}, t)\\ &- \mathbf{H}_{21}(\bar{\boldsymbol{\theta}}, 0)\mathbf{g}_1(\bar{\boldsymbol{\theta}}, \dot{\bar{\boldsymbol{\theta}}}, 0, 0, t) + \mathbf{H}_{21}(\bar{\boldsymbol{\theta}}, 0)\bar{\mathbf{T}}\big]\\ &- \mathbf{f}_2(\bar{\boldsymbol{\theta}}, \dot{\bar{\boldsymbol{\theta}}}, t) - \mathbf{g}_2(\bar{\boldsymbol{\theta}}, \dot{\bar{\boldsymbol{\theta}}}, 0, 0, t),\end{aligned} \tag{12}$$

where the overbars are used to indicate that the system with $\mu = 0$ is considered. Plugging (12) into (11a) yields

$$\begin{aligned}\ddot{\bar{\boldsymbol{\theta}}} = &\big[\mathbf{H}_{11}(\bar{\boldsymbol{\theta}}, 0) - \mathbf{H}_{12}(\bar{\boldsymbol{\theta}}, 0)\mathbf{H}_{22}^{-1}(\bar{\boldsymbol{\theta}}, 0)\mathbf{H}_{21}(\bar{\theta}, 0)\big]\\ &\times \big[-\mathbf{f}_1(\bar{\boldsymbol{\theta}}, \dot{\bar{\boldsymbol{\theta}}}, t) + \bar{\mathbf{T}}\big],\end{aligned} \tag{13}$$

where

$$\mathbf{H}_{11}(\bar{\boldsymbol{\theta}}, 0) - \mathbf{H}_{12}(\bar{\boldsymbol{\theta}}, 0)\mathbf{H}_{22}^{-1}(\bar{\boldsymbol{\theta}}, 0)\mathbf{H}_{21}(\bar{\boldsymbol{\theta}}, 0) = \mathbf{M}_{11}^{-1}(\bar{\boldsymbol{\theta}}) \tag{14}$$

and where $\mathbf{M}^{rr}(\bar{\boldsymbol{\theta}})$ is the $[n \times n]$ positive definite matrix for the rigid-link arm.

Choosing $\mathbf{x}_1 = \boldsymbol{\theta}$, $\mathbf{x}_2 = \dot{\boldsymbol{\theta}}$, and $\mathbf{z}_1 = \boldsymbol{\zeta}$, and $\mathbf{z}_2 = \varepsilon\dot{\boldsymbol{\zeta}}$ with $\varepsilon = \sqrt{\mu}$ gives the state-space form of the system (11a)–(11b), i.e.,

$$\begin{aligned}\dot{\mathbf{x}}_1 &= \mathbf{x}_2,\\ \dot{\mathbf{x}}_2 &= -\mathbf{H}_{11}\big(\mathbf{x}_1, \varepsilon^2\mathbf{z}_1\big)\mathbf{f}_1(\mathbf{x}_1, \mathbf{x}_2, t)\\ &\quad - \mathbf{H}_{12}\big(\mathbf{x}_1, \varepsilon^2\mathbf{z}_1\big)\mathbf{f}_2(\mathbf{x}_1, \mathbf{x}_2, t)\\ &\quad - \mathbf{H}_{11}\big(\mathbf{x}_1, \varepsilon^2\mathbf{z}_1\big)\mathbf{g}_1\big(\mathbf{x}_1, \mathbf{x}_2, \varepsilon^2\mathbf{z}_1, \varepsilon\mathbf{z}_2, t\big)\\ &\quad - \mathbf{H}_{12}\big(\mathbf{x}_1, \varepsilon^2\mathbf{z}_1\big)\mathbf{g}_2\big(\mathbf{x}_1, \mathbf{x}_2, \varepsilon^2\mathbf{z}_1, \varepsilon\mathbf{z}_2, t\big)\\ &\quad - \mathbf{H}_{12}\big(\mathbf{x}_1, \varepsilon^2\mathbf{z}_1\big)\mathbf{z}_1 + \mathbf{H}_{11}\big(\mathbf{x}_1, \varepsilon^2\mathbf{z}_1\big)\mathbf{T},\end{aligned} \tag{15a}$$

$$\begin{aligned}\varepsilon\dot{\mathbf{z}}_1 &= \mathbf{z}_2,\\ \varepsilon\dot{\mathbf{z}}_2 &= -\mathbf{H}_{21}\big(\mathbf{x}_1, \varepsilon^2\mathbf{z}_1\big)\mathbf{f}_1(\mathbf{x}_1, \mathbf{x}_2, t)\\ &\quad - \mathbf{H}_{22}\big(\mathbf{x}_1, \varepsilon^2\mathbf{z}_1\big)\mathbf{f}_2(\mathbf{x}_1, \mathbf{x}_2, t)\\ &\quad - \mathbf{H}_{21}\big(\mathbf{x}_1, \varepsilon^2\mathbf{z}_1\big)\mathbf{g}_1\big(\mathbf{x}_1, \mathbf{x}_2, \varepsilon^2\mathbf{z}_1, \varepsilon\mathbf{z}_2, t\big)\\ &\quad - \mathbf{H}_{22}\big(\mathbf{x}_1, \varepsilon^2\mathbf{z}_1\big)\mathbf{g}_2\big(\mathbf{x}_1, \mathbf{x}_2, \varepsilon^2\mathbf{z}_1, \varepsilon\mathbf{z}_2, t\big)\\ &\quad - \mathbf{H}_{22}\big(\mathbf{x}_1, \varepsilon^2\mathbf{z}_1\big)\mathbf{z}_1 + \mathbf{H}_{21}\big(\mathbf{x}_1, \varepsilon^2\mathbf{z}_1\big)\mathbf{T}.\end{aligned} \tag{15b}$$

At this point, the slow subsystem is obtained by setting $\varepsilon = 0$:

$$\begin{aligned}\dot{\bar{\mathbf{x}}}_1 &= \bar{\mathbf{x}}_2,\\ \dot{\bar{\mathbf{x}}}_2 &= \mathbf{M}_{11}^{-1}(\bar{\mathbf{x}}_1)\big[-\mathbf{f}_1(\bar{\mathbf{x}}_1, \bar{\mathbf{x}}_2, t) + \mathbf{T}\big].\end{aligned} \tag{16}$$

To derive the fast subsystem, we introduce the fast time scale $\tau = t/\varepsilon$. Then it can be recognized that the system (15a)–(15b) in the fast time scale becomes

$$\begin{aligned}\frac{d\mathbf{x}_1}{d\tau} &= \varepsilon\mathbf{x}_2,\\ \frac{d\mathbf{x}_2}{d\tau} &= \varepsilon\big[-\mathbf{H}_{11}\big(\mathbf{x}_1, \varepsilon^2(\boldsymbol{\eta}_1 + \bar{\boldsymbol{\zeta}})\big)\mathbf{f}_1(\mathbf{x}_1, \mathbf{x}_2, t)\\ &\quad - \mathbf{H}_{12}\big(\mathbf{x}_1, \varepsilon^2(\boldsymbol{\eta}_1 + \bar{\boldsymbol{\zeta}})\big)\mathbf{f}_2(\mathbf{x}_1, \mathbf{x}_2, t)\\ &\quad - \mathbf{H}_{11}\big(\mathbf{x}_1, \varepsilon^2(\boldsymbol{\eta}_1 + \bar{\boldsymbol{\zeta}})\big)\\ &\quad \times \mathbf{g}_1\big(\mathbf{x}_1, \mathbf{x}_2, \varepsilon^2(\boldsymbol{\eta}_1 + \bar{\boldsymbol{\zeta}}), \varepsilon\boldsymbol{\eta}_2, t\big)\\ &\quad - \mathbf{H}_{12}\big(\mathbf{x}_1, \varepsilon^2(\boldsymbol{\eta}_1 + \bar{\boldsymbol{\zeta}})\big)\\ &\quad \times \mathbf{g}_2\big(\mathbf{x}_1, \mathbf{x}_2, \varepsilon^2(\boldsymbol{\eta}_1 + \bar{\boldsymbol{\zeta}}), \varepsilon\boldsymbol{\eta}_2, t\big)\\ &\quad - \mathbf{H}_{12}\big(\mathbf{x}_1, \varepsilon^2(\boldsymbol{\eta}_1 + \bar{\boldsymbol{\zeta}})\big)(\boldsymbol{\eta}_1 + \bar{\boldsymbol{\zeta}})\\ &\quad + \mathbf{H}_{11}\big(\mathbf{x}_1, \varepsilon^2(\boldsymbol{\eta}_1 + \bar{\boldsymbol{\zeta}})\big)\mathbf{T}\big],\end{aligned} \tag{17a}$$

$$
\begin{aligned}
\frac{d\boldsymbol{\eta}_1}{d\tau} &= \boldsymbol{\eta}_2,\\
\frac{d\boldsymbol{\eta}_2}{d\tau} &= -\mathbf{H}_{21}\big(\mathbf{x}_1, \varepsilon^2(\boldsymbol{\eta}_1+\bar{\boldsymbol{\zeta}})\big)\mathbf{f}_1(\mathbf{x}_1,\mathbf{x}_2,t)\\
&\quad -\mathbf{H}_{22}\big(\mathbf{x}_1, \varepsilon^2(\boldsymbol{\eta}_1+\bar{\boldsymbol{\zeta}})\big)\mathbf{f}_2(\mathbf{x}_1,\mathbf{x}_2,t)\\
&\quad -\mathbf{H}_{21}\big(\mathbf{x}_1, \varepsilon^2(\boldsymbol{\eta}_1+\bar{\boldsymbol{\zeta}})\big)\\
&\quad \times \mathbf{g}_1\big(\mathbf{x}_1,\mathbf{x}_2, \varepsilon^2(\boldsymbol{\eta}_1+\bar{\boldsymbol{\zeta}}), \varepsilon\boldsymbol{\eta}_2, t\big)\\
&\quad -\mathbf{H}_{22}\big(\mathbf{x}_1, \varepsilon^2(\boldsymbol{\eta}_1+\bar{\boldsymbol{\zeta}})\big)\\
&\quad \times \mathbf{g}_2\big(\mathbf{x}_1,\mathbf{x}_2, \varepsilon^2(\boldsymbol{\eta}_1+\bar{\boldsymbol{\zeta}}), \varepsilon\boldsymbol{\eta}_2, t\big)\\
&\quad -\mathbf{H}_{22}\big(\mathbf{x}_1, \varepsilon^2(\boldsymbol{\eta}_1+\bar{\boldsymbol{\zeta}})\big)(\boldsymbol{\eta}_1+\bar{\boldsymbol{\zeta}})\\
&\quad +\mathbf{H}_{21}\big(\mathbf{x}_1, \varepsilon^2(\boldsymbol{\eta}_1+\bar{\boldsymbol{\zeta}})\big)\mathbf{T},
\end{aligned}
\tag{17b}
$$

where the new fast variables $\boldsymbol{\eta}_1$ and $\boldsymbol{\eta}_2$ are defined as

$$
\boldsymbol{\eta}_1 = \mathbf{z}_1 - \bar{\boldsymbol{\zeta}} = \mathbf{z}_1 - \bar{z}_1, \qquad \boldsymbol{\eta}_2 = \mathbf{z}_2. \tag{18}
$$

Now setting $\varepsilon = 0$ in (17a) and (17b) gives $\frac{d\mathbf{x}_1}{d\tau} = \frac{d\mathbf{x}_2}{d\tau} = 0$, i.e., $\mathbf{x}_1$ and $\mathbf{x}_2$ are constants. Furthermore, it can be recognized that $\mathbf{g}_1(\mathbf{x}_1,\mathbf{x}_2,0,0) = 0$ and $\mathbf{g}_2(\mathbf{x}_1,\mathbf{x}_2,0,0) = 0$ since those terms are representative of products of the components of $\mathbf{x}_1$ and/or $\mathbf{x}_2$ with the components of $\varepsilon^2\mathbf{z}_1$ and/or $\varepsilon\mathbf{z}_2$. Therefore, the fast subsystem can be found to be

$$
\begin{aligned}
\frac{d\boldsymbol{\eta}_1}{d\tau} &= \boldsymbol{\eta}_2,\\
\frac{d\boldsymbol{\eta}_2}{d\tau} &= -\mathbf{H}_{22}(\bar{\mathbf{x}}_1,0)\boldsymbol{\eta}_1 + \mathbf{H}_{21}(\bar{\mathbf{x}}_1,0)(\mathbf{T}-\bar{\mathbf{T}}),
\end{aligned}
\tag{19}
$$

which is a linear system parameterized in the slow variables $\bar{\mathbf{x}}_1$.

3.2 Composite control

As evidenced by the two reduced-order subsystems (16) and (19), a composite control strategy can now be pursued. The design of a feedback control for the full system can be split into two separated designs of feedback controls $\bar{\mathbf{T}}$ and $\mathbf{T}_f$ for the two reduced-order systems; formally,

$$
\mathbf{T} = \bar{\mathbf{T}}(\bar{\mathbf{x}}_1,\bar{\mathbf{x}}_2,t) + \mathbf{T}_f(\bar{\mathbf{x}}_1,\boldsymbol{\eta}_1,\boldsymbol{\eta}_2), \tag{20}
$$

where $\bar{\mathbf{T}}(\bar{\mathbf{x}}_1,\bar{\mathbf{x}}_2,t)$ is the slow control, and $\mathbf{T}_f(\bar{\mathbf{x}}_1,\boldsymbol{\eta}_1,\boldsymbol{\eta}_2)$ is the fast control.

As far as the slow control is concerned, the computed torque control developed for rigid manipulators as shown previously can be utilized and the slow control is given by (7).

At this point, the fast subsystem (19) is required to be uniformly stable along the equilibrium trajectory $\bar{\boldsymbol{\zeta}}$ given by (12). This can be accomplished if the pair

$$
\mathbf{A} = \begin{bmatrix} \mathbf{0} & \mathbf{I} \\ -\mathbf{H}_{22} & \mathbf{0} \end{bmatrix}, \qquad \mathbf{B} = \begin{bmatrix} \mathbf{0} \\ \mathbf{H}_{21} \end{bmatrix} \tag{21}
$$

is stabilizable for any slow trajectory $\bar{\mathbf{x}}_1(t)$. Assuming that this holds, a fast state feedback control of the type

$$
\mathbf{T}_f = \mathbf{k}_{pf}(\bar{\mathbf{x}}_1)\boldsymbol{\eta}_1 + \mathbf{k}_{vf}(\bar{\mathbf{x}}_1)\boldsymbol{\eta}_2 \tag{22}
$$

will stabilize the fast subsystem (19) to $\boldsymbol{\eta}_1 = 0$ ($\mathbf{z}_1 = \bar{\boldsymbol{\zeta}}$) and $\boldsymbol{\eta}_2 = 0$ ($\mathbf{z}_2 = 0$). Since the main purpose of flexible manipulator control is to damp out the deflections at steady state as fast as possible, the fast control (22) can be designed following optimal control techniques.

Under the above conditions, the state vectors of the full system can be approximated by

$$
\mathbf{x}_1 = \bar{\mathbf{x}}_1 + \mathbf{O}(\varepsilon), \qquad \mathbf{x}_2 = \bar{\mathbf{x}}_2 + \mathbf{O}(\varepsilon), \tag{23a}
$$

$$
\mathbf{z}_1 = \bar{\boldsymbol{\zeta}} + \boldsymbol{\eta}_1 + \mathbf{O}(\varepsilon), \qquad \mathbf{z}_2 = \boldsymbol{\eta}_2 + \mathbf{O}(\varepsilon), \tag{23b}
$$

where the operator $\mathbf{O}(\varepsilon)$ means the order of magnitude of ε. Under the slow control (11), $\boldsymbol{\theta}$ and $\dot{\boldsymbol{\theta}}$ will tend to $\boldsymbol{\theta}_d$ and $\dot{\boldsymbol{\theta}}_d$, respectively. The fast control (22) will derive $\boldsymbol{\eta}_1$ and $\boldsymbol{\eta}_2$ to zero.

4 Numerical example

A one-link flexible arm shown in Fig. 2, subjected to parametric excitation, is commanded to follow a

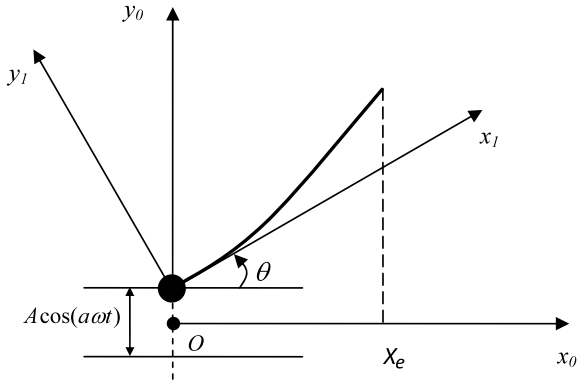

Fig. 2 One-link flexible-arm schematic

certain trajectory under the control of both computed torque and composite control. The beam used is made of stainless steel with $m = 0.075$ kg, $L = 0.3$ m, and $EI = 40$ N m^2. The deformation of the arm is described by the first two bending modes since the higher bending modes are observed to be negligible. The base of the manipulator is excited with the function $A\cos(a\omega t)$, where $a = 1/5$ is the excitation frequency coefficient, $\omega = 400$ rad/s is the smallest natural frequency of the beam, $A = 0.05$ m is the amplitude of excitation. A step change from $\theta = 0°$ to $\theta = 90°$ is assigned to the joint angle. The performance of the manipulator under the composite control and under the computed torque control is investigated.

The gains of the computed torque control are obtained as $k_p = 12.25$ and $k_v = 7$. The gains used to calculate the fast control torque (22) are obtained based on the Linear Quadratic Regulator (LQR) control technique [15], where the performance measures are achieved by selecting the weighing matrices of the regulator $\mathbf{Q}$ and $\mathbf{R}$ as $\mathbf{Q} = 30\mathbf{I}$ and $\mathbf{R} = 5\mathbf{I}$.

The perturbation parameter value used in the following simulations, as justified later, is $\mu = 1/k_1 = 0.0003$. Figures 3 and 4 show the response of the first modal variable δ_1 under both computed torque and composite control, respectively. The results show that a valuable improvement of the first modal variable response is achieved by the composite control over the computed torque control. The order of magnitude of the first modal variable, in the case of composite control, is one-half that in the case of computed torque control. And the response settling time is tremendously reduced under the composite control.

In Figs. 5 and 6, the response of the second modal variable δ_2 is presented. The results again show that the amplitude of oscillations, in the case of composite control, is of the order of magnitude of one-half that of computed torque control with better settling time. This improvement in response is based on the composite control strategy for trajectory tracking which exploits the two-time scale nature of the flexible part and the rigid part of the dynamic equations.

Figure 7 shows the response of the joint angle under the computed torque control and the composite control, where the response in the two cases is nearly the same.

The control signals and hence torques were devised such that both control techniques have the same joint angle settling time.

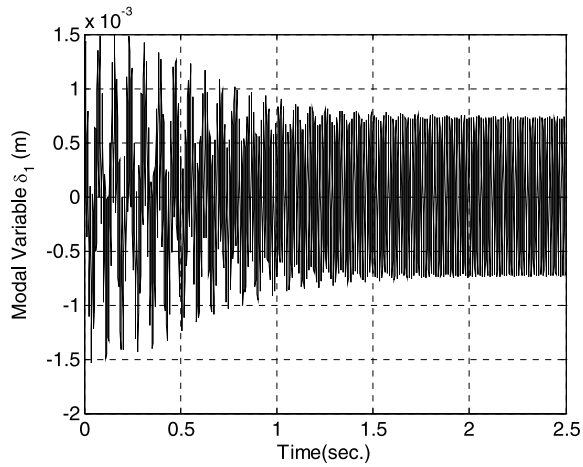

Fig. 3 First modal variable δ_1 (computed torque control)

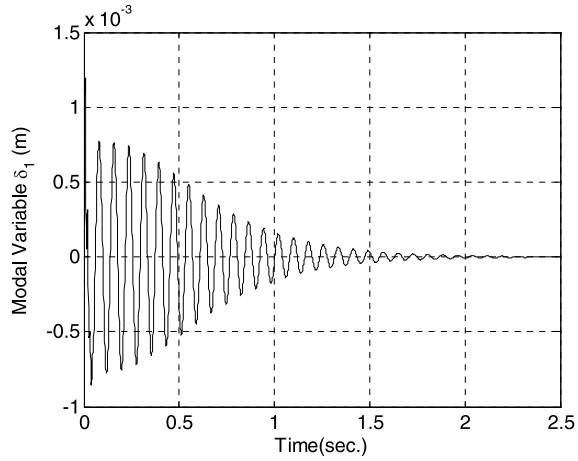

Fig. 4 First modal variable δ_1 (composite control)

At this step, the composite control algorithm is applied to the manipulator with different values of the perturbation parameter μ. The response of the manipulator is then investigated utilizing three values of the perturbation parameter. It is observed that the only term affected by changing the value of this parameter is the control torque shown in Fig. 8. The minimum control torque effort required by the motor is achieved as $\mu = 1/k_1 = 0.0003$, and for the two other values $\mu = 0.0001$ and $\mu = 0.001$, the control effort required is observed to be higher. This is due to the fact that the value of the perturbation parameter affects the fast subsystem dynamics (21). Hence, the gains required to place the eigenvalues of the fast subsystem are different for different μ's which, in turn, affects the value

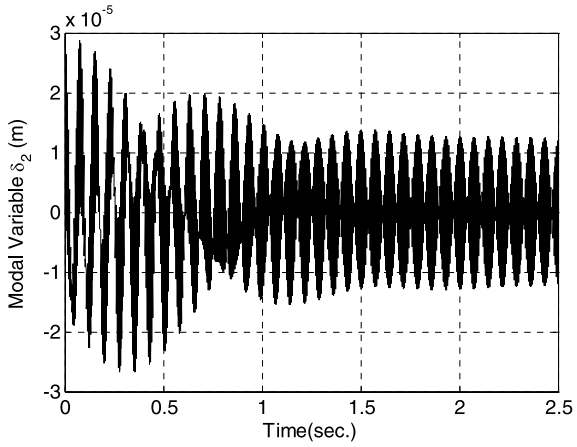

Fig. 5 Second modal variable δ_2 (computed torque control)

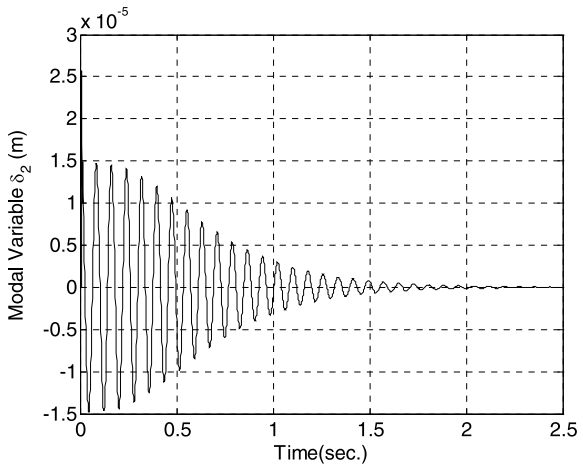

Fig. 6 Second modal variable δ_2 (composite control)

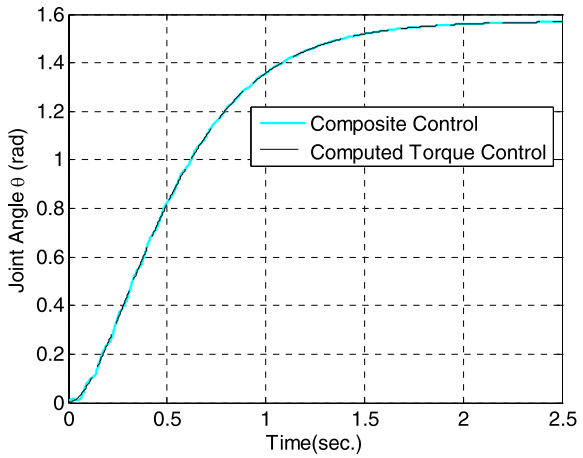

Fig. 7 Joint angle

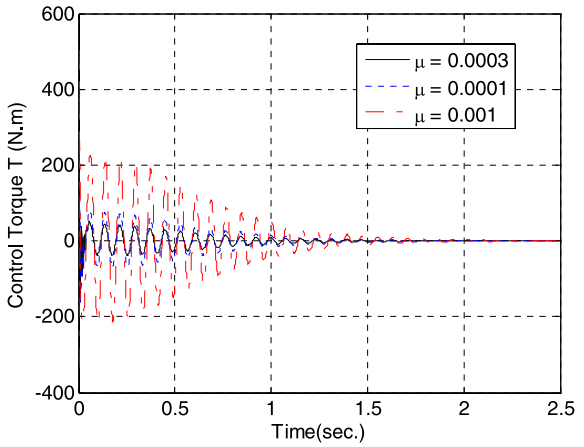

Fig. 8 Control torque for different μ's (composite control)

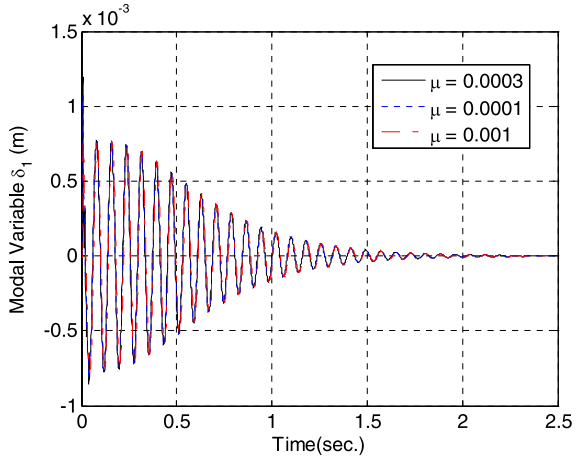

Fig. 9 First modal variable δ_1 for different μ's (composite control)

of the control torque required. On the other hand, the response of the first modal variable δ_1 has not been affected by the value of the perturbation parameter as shown in Fig. 9 since the eigenvalues were placed at the same location for all μ's used. These curves again show that the optimum perturbation parameter value to be used is $\mu = 1/k_1$ where k_1 is the smallest stiffness value in the stiffness matrix.

5 Experimental study

In this section, experimental study is carried out to demonstrate the effectiveness of the proposed method on a physical system and thus verify theoretical results. The testbed consists of a DC motor equipped

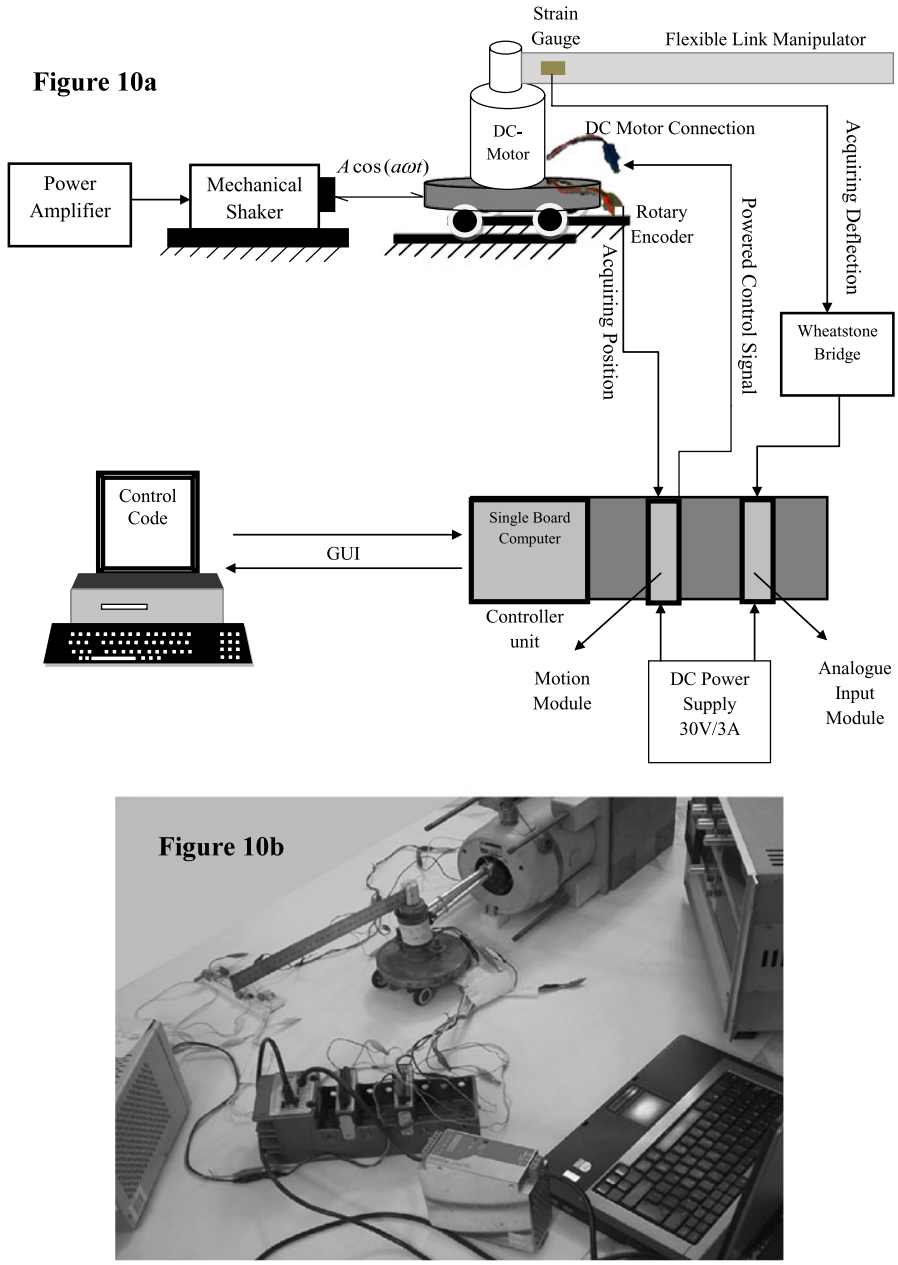

Fig. 10 Experimental setup: (**a**) schematic diagram, (**b**) testbed

with an optical encoder, 0.3 m long flexible manipulator with an attached strain gauge, an electrodynamic shaker, real-time controller and an amplifier module. A schematic of the experimental setup and the testbed are shown Fig. 10.

Figures 11 and 12 show the link deflections under the computed torque control and composite control, respectively. It can be observed that experimental measurements match those of the theoretical results obtained earlier. Here the perturbation parameter used is $\mu = 0.0003$ which is the theoretically determined to be the optimum value.

Figure 13 shows the joint response under both computed torque control and composite control which are similar to those obtained numerically. Hence theoretical results are verified experimentally.

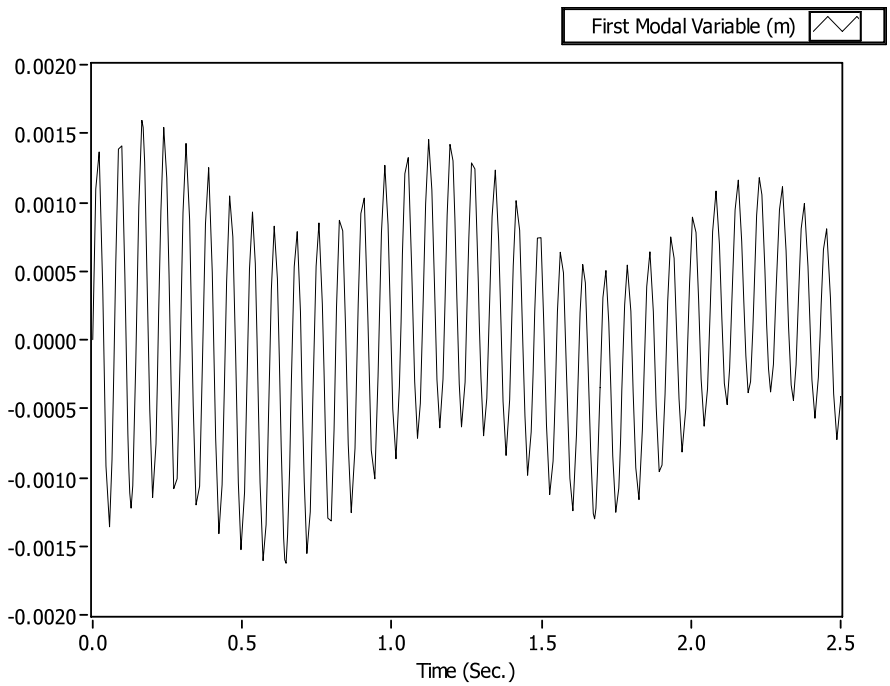

Fig. 11 First modal variable δ_1 (computed torque control)

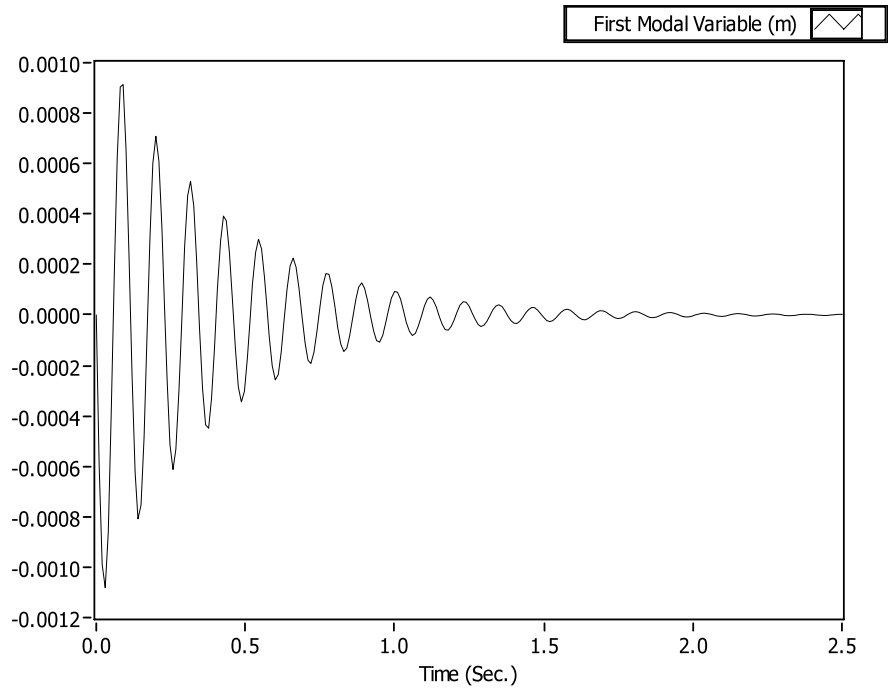

Fig. 12 First modal variable δ_1 (composite control)

6 Conclusion

In this study, the nonlinear time-varying dynamic equations of motion of flexible-link manipulators subjected to parametric excitation were derived. In contrast to the external excitation, the parametric excitation leads to equations of motion with rapidly varying coefficients. The response of such systems while

Fig. 13 Joint angle

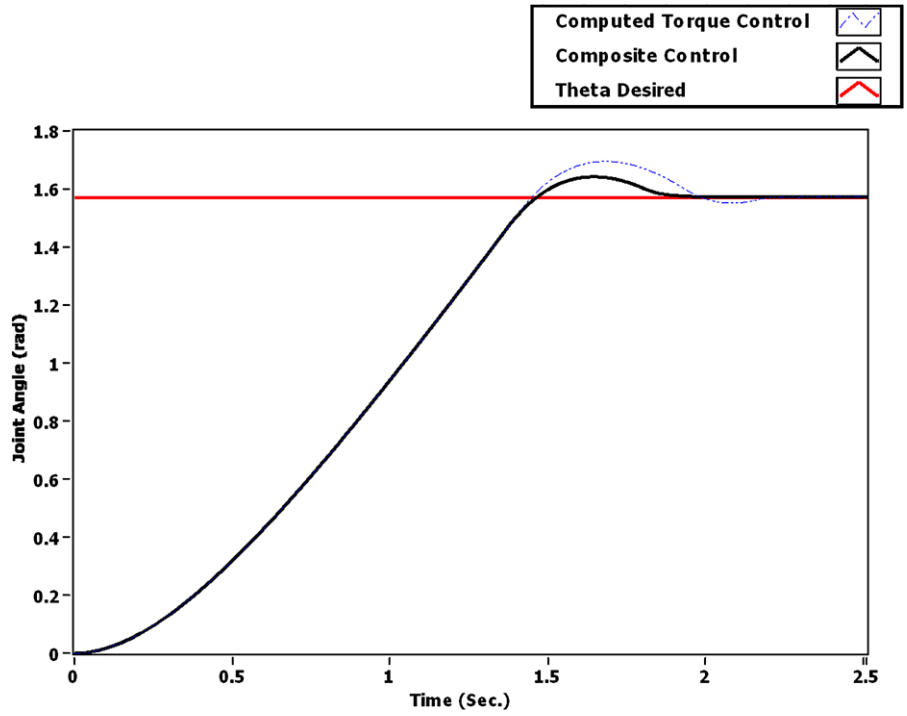

tracking a certain trajectory is investigated under the control of both computed torque and a composite control based on a developed singular perturbation method. The effect of the perturbation parameter used has been investigated and an optimal value has been determined. Both numerical simulations and experimental measurements show better system response under the composite control technique.

Appendix

The fixed-free deflection modes are [16]:

$$\phi_j(x) = \left(\sin\frac{a_j x}{L} - \sinh\frac{a_j x}{L}\right) - \frac{(\sin a_j + \sinh a_j)}{(\cos a_j + \cosh a_j)} \times \left(\cos\frac{a_j x}{L} - \cosh\frac{a_j x}{L}\right), \tag{A.1}$$

for $j = 1, 2, a_1 = 1.875$ and $a_2 = 4.694$.

The equations of motions of a one link flexible arm can be written in the following form:

$$\begin{bmatrix} M_{11} & M_{12} & M_{13} \\ M_{21} & M_{22} & M_{23} \\ M_{31} & M_{32} & M_{33} \end{bmatrix} \begin{bmatrix} \ddot{\theta} \\ \ddot{\delta}_1 \\ \ddot{\delta}_2 \end{bmatrix} + \begin{bmatrix} f_1 \\ f_{21} \\ f_{22} \end{bmatrix} + \begin{bmatrix} g_1 \\ g_{21} \\ g_{22} \end{bmatrix} + \begin{bmatrix} 0 \\ K\begin{bmatrix} \delta_1 \\ \delta_2 \end{bmatrix} \end{bmatrix} = \begin{bmatrix} T_1 \\ 0 \\ 0 \end{bmatrix}, \tag{A.2}$$

where the elements of the previous equation are given as:

$$M_{11} = J_h + \frac{1}{3}mL^2, \tag{A.3}$$

$$M_{12} = 0.7748m, \tag{A.4}$$

$$M_{13} = 0.08916m, \tag{A.5}$$

$$M_{21} = M_{12}, \tag{A.6}$$

$$M_{22} = 1.85534m, \tag{A.7}$$

$$M_{23} = 0.0001m, \tag{A.8}$$

$$M_{31} = M_{13}, \tag{A.9}$$

$$M_{32} = M_{23}, \tag{A.10}$$

$$M_{33} = 0.964m, \tag{A.11}$$

$$\mathbf{f}_1 = f_1 = -0.5a^2 ALm\omega^2 \cos(a\omega t)\cos(\theta), \tag{A.12}$$

$$\mathbf{f}_2 = \begin{bmatrix} f_{21} \\ f_{22} \end{bmatrix}, \tag{A.13}$$

where

$$f_{21} = -1.06652a^2 Am\omega^2 \cos(a\omega t)\cos(\theta), \tag{A.14}$$

$$f_{22} = -0.426a^2 Am\omega^2 \cos(a\omega t)\cos(\theta), \tag{A.15}$$

$$\mathbf{g}_1 = g_1 = 1.06652a^2 Am\omega^2 \cos(a\omega t)\sin(\theta)\delta_1 + 0.4261a^2 Am\omega^2 \cos(a\omega t)\sin(\theta)\delta_2, \tag{A.16}$$

$$\mathbf{g}_2 = \begin{bmatrix} g_{21} \\ g_{22} \end{bmatrix}, \tag{A.17}$$

with

$$g_{21} = -1.8553m\delta_1\dot{\theta}^2 - 0.0001m\delta_2\dot{\theta}^2, \tag{A.18}$$

$$g_{22} = -0.0001m\delta_1\dot{\theta}^2 - 0.964m\delta_2\dot{\theta}^2, \tag{A.19}$$

$$\mathbf{K} = \begin{bmatrix} 22.93\frac{EI}{L^3} & 0 \\ 0 & 468.04\frac{EI}{L^3} \end{bmatrix} \tag{A.20}$$

where beam mass $m = 0.075$ kg, joint inertia $J_h = 0.5\ \mathrm{kg\,m^2}$, beam length $L = 0.3$ m, and flexural rigidity $EI = 40\ \mathrm{N\,m^2}$.

References

1. Nayfeh, A.H., Mook, D.T.: Nonlinear Oscillations. Wiley, New York (1979)
2. Lin, J., Huang, Z.Z., Huang, P.H.: An active damping control of robot manipulators with oscillatory bases by singular perturbation approach. J. Sound Vib. **304**, 345–360 (2007)
3. Lew, J.Y., Moon, S.: A simple active damping control for compliant base manipulators. Mechatronics **6**(3), 305–310 (2001)
4. Lin, J., Huang, Z.Z.: A hierarchical fuzzy approach to supervisory control of robot manipulators with oscillatory bases. Mechatronics **17**(10), 589–600 (2007)
5. Mohamed, Z., Martins, J.M., Tokhi, M.O., da Costa, J., Botto, M.: Vibration control of a very flexible manipulator system. Control Eng. Pract. **13**, 267–277 (2005)
6. Subudhi, B., Morris, A.S.: On the singular perturbation approach to trajectory control of a multilink manipulator with flexible links and joints. J. Syst. Control Eng. **215**(6), 587–598 (2001)
7. Dwivedy, S.K., Eberhard, P.: Dynamic analysis of flexible manipulators, a literature review. Mech. Mach. Theory **41**, 749–777 (2006)
8. Ider, S., Ozgoren, M., Ay, V.: Trajectory tracking control of robots with flexible links. Mech. Mach. Theory **37**, 1377–1394 (2002)
9. Siciliano, B., Book, W.J.: A singular perturbation approach to control of lightweight flexible manipulators. Int. J. Robot. Res. **7**(4), 79–90 (1988)
10. Spong, M., Hutchinson, S., Vidyasagar, M.: Robot Modeling and Control. Wiley, New York (2006)
11. Nayfeh, A.H.: Introduction to Perturbation Techniques. Wiley, New York (1981)
12. Book, W.J.: Recursive Lagrangian dynamics of flexible manipulator arms via transformation matrices. Int. J. Robot. Res. **3**(3), 87–101 (1984)
13. De Luca, A., Siciliano, B.: Closed-form dynamic model of planar multilink lightweight robots. IEEE Trans. Syst. Man Cybern. **21**(4), 826–839 (1991)
14. Kokotovic, P.V.: Applications of singular perturbation techniques to control problems. Soc. Ind. Appl. Math. **26**(4), 501–550 (1984)
15. Ogata, K.: Modern Control Engineering, 5th edn. Pearson, Upper Saddle River (2010)
16. Meirovitch, L.: Fundamentals of Vibrations. McGraw-Hill, New York (2001)